IOSR Journal of Applied Physics (IOSR-JAP)
e-ISSN: 2278-4861.Volume 9, Issue 4 Ver. III (Jul. – Aug. 2017), PP 57-67
www.iosrjournals.org

Growth, Structural, Optical, Thermal and Mechanical properties of Copper Glutamate Dihydrate Single crystal

S. Sakthivel[a], T. Balakrishnan[b,]*, P. Revathi[b], and P. Jaikumar[c]
[1]*PG & Research Department of Physics, Govt. Arts College (Autonomous), Karur – 639 005, Tamil Nadu, India*
[2]*Crystal Growth Laboratory, PG & Research Department of Physics, Periyar E.V.R. College (Autonomous), Tiruchirappalli – 620 023, Tamil Nadu, India.*
[3]*PG& Research Department of Physics, National College, Tiruchirappalli – 620 001, Tamil Nadu, India.*
Corresponding Author: S. Sakthivel

Abstract: *Semiorganic nonlinear optical single crystals of copper glutamate dihydrate ($CuC_5H_7NO_4.2H_2O$) were grown by slow evaporation technique at room temperature. Single crystal X - ray diffraction analysis reveals that the grown crystal belongs to orthorhombic system with space group $P2_12_12_1$. The crystallinity of the grown crystals was studied by powder X - ray diffraction analysis and their diffraction pattern was indexed using AUTOX 93 software. Functional groups of synthesized material was identified using Fourier transform infrared (FT – IR) spectroscopic analysis. The optical transmission percentage of grown CLGD crystal was ascertained by UV – Vis – NIR spectrum. The photoluminescence spectrum shows an emission peak at 555 nm using the excitation wavelength of 275 nm. The mechanical strength of the grown crystal was determined using Vickers microhardness tester. Electrical properties were analyzed by dielectric measurement at different temperatures. Thermal stability of the grown crystal was studied by thermogravimetric, differential thermal analysis and differential scanning calorimetry. Etching study was carried out to assess the perfection of the grown crystals. The second harmonic generation efficiency was calculated by Kurtz and Perry powder technique.*

Keywords: *Crystal growth, Mechanical strength, Thermal properties, Optical properties.*

Date of Submission: 18-07-2017 Date of acceptance: 10-08-2017

I. Introduction

L-glutamic acid is a dicarboxylic amino acid and is a significant constituent in proteins. It also plays an important role in the metabolism of sugar and fats. L-glutamic acid crystallizes in two polymorphs one a metastable α and a stable β which has different lattice parameters of the same space group of the orthorhombic $P2_12_12_1$. The α form of L - glutamic acid structure was published by Bernal [1] and the β polymorph was reported by Hirokawa [2]. The kinetics of polymorphic transformation between α and β forms of L glutamic acid was observed [3]. The metastable α form is easily grown and poor conformational discrimination at the (111) faces favours surface nucleation of β form. Crystals of α form are rhombic whereas the β polymorph forms needle like crystals [4]. Crystal structures of L - glutamic acid hydrochloride [5], DL glutamic acid hydrochloride [6], anhydrous DL glutamic acid [7] and bis L - glutamic acid sulphate hemihydrate [8] have been reported. Due to the inherent limitations of organic and inorganic single crystal researchers developed a new hybrid crystals containing organic and metals. With the aim of growing efficient NLO crystals various groups have published several salts and mixed salts of L – glutamic acid [9 - 12]. The crystal structure of copper L - glutamate dihydrate was first reported by Gramaccioli and Marsh [13]. Orthorhombic crystals of CLGD crystallizes in a noncentrosymmetric structure with lattice dimensions a = 11084 Å, b = 10.350 Å and c = 7.235Å. In this study we report the results of single crystal growth of copper L - glutamate dihydrate and characterization studies of its linear and nonlinear optical, spectroscopic, photoluminescence, mechanical, dielectric and thermal stability.

II. Experimental Procedure

2.1 Synthesis

Copper L glutamate dihydrate salt was synthesized by mixing L – Glutamic acid 99% purity and copper (II) hydroxide carbonate purchased from Merck were taken in 1:1 equimolar ratio. L - Glutamic acid was dissolved completely at 35 ^{0} C in double distilled water then Copper (II) hydroxide carbonate is mixed. The solution was thoroughly stirred and few drops of HNO_3 are added for complete dissolution. The prepared solution was constantly stirred about 3 hours using magnetic stirrer to obtain homogeneous mixture over the

entire volume. The salt was obtained after a week by slow evaporation. To ensure high purity, the material was purified by successive recrystallization. The single crystal growth was achieved by dissolving the synthesized polycrystalline salts in double distilled water to form saturation solution. The solution was filtered twice to remove the impurities using Whatman filter paper and kept in a borosil beaker covered with porous paper to facilitate the evaporation of the solvent. The crystals of optimum size (6×6×3) mm^3 were obtained after a period of 15 days. The photograph of grown crystals of copper L-glutamate dihydrate is shown in Fig. 1.

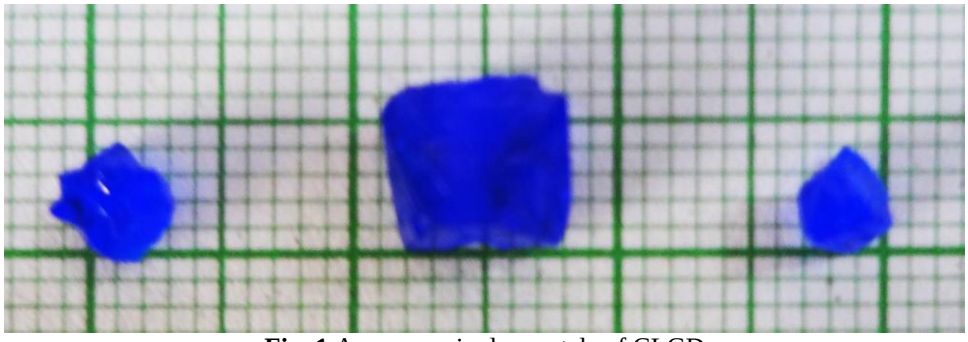

Fig. 1 As grown single crystals of CLGD

III. Results And Discussion

3.1 Single crystal X – ray diffraction

The structure of the grown single crystal was confirmed by single crystal X-ray diffraction analysis using ENRAF CAD4 diffractometer with MoKα radiation. The structure was solved by direct method and refined by full matrix least squares refinements using SHELXL program. CLGD crystallizes in orthorhombic system with noncentrosymmetric space group $P2_12_12_1$. The lattice parameters obtained from single crystal X – ray diffraction analysis are presented in Table 1. Fig. 2 shows the molecular ORTEP diagram of CLGD. The coordination of copper atom is approximately square planar, the square comprising of two oxygen atoms and a nitrogen atom of glutamate groups and a water molecule. The average distance from the copper atom to these four ligands is 2.056 Å. The nitrogen atom is tetra coordinated and the Cu – O and Cu – N distances range from 1.9656 to 1.9946 Å.

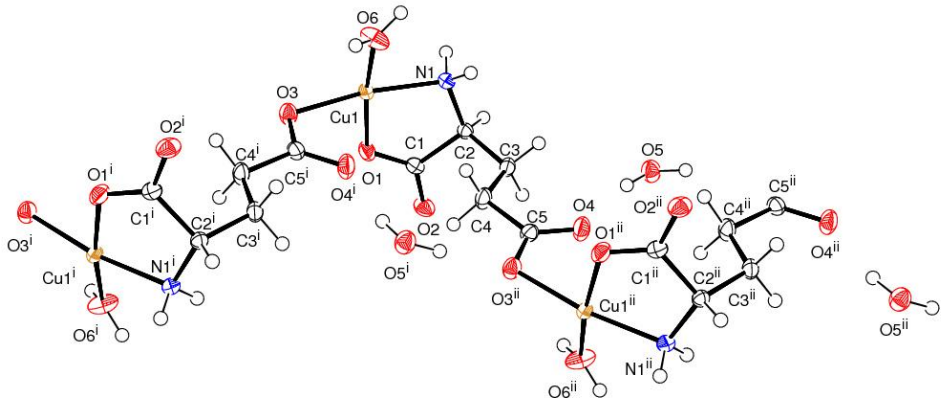

Fig. 2 ORTEP diagram of CLGD

TABLE 1 Crystal Data and Structure Refinement for CLGD

Empirical formula	$C_5 H_{11} Cu N O_6$
Formula weight	244.69
Temperature	296(2) K
Wavelength	0.71073 A
Crystal system, space group	Orthorhombic, $P2_12_12_1$
Unit cell dimensions	a = 7.2248(3) Å α = 90 deg. b = 10.2992(5) Å β = 90 deg c = 11.0453(5) Å γ = 90 deg.
Volume	821.88(6) A^3
Z, Calculated density	4, 1.977 Mg/m^3
Absorption coefficient	2.657 mm^-1
F (000)	500
Crystal size	0.35 x 0.32 x 0.30 mm

Theta range for data collection	2.70 to 26.96 deg.
Limiting indices	-9<=h<=8, -13<=k<=13, -14<=l<=14
Reflections collected / unique	13523 / 1787 [R(int) = 0.0302]
Completeness to theta = 26.96	100.0 %
Absorption correction	Semi-empirical from equivalents
Max. and min. transmission	0.5096 and 0.4514
Refinement method	Full-matrix least-squares on F^2
Data / restraints / parameters	1787 / 9 / 143
Goodness-of-fit on F^2	1.141
Final R indices [I>2 sigma (I)]	R1 = 0.0133, wR2 = 0.0363
R indices (all data)	R1 = 0.0140, wR2 = 0.0367
Absolute structure parameter	-0.008(9)
Extinction coefficient	0.0405(14)
Largest diff. peak and hole	0.239 and -0.249 e.A^-3

3.2 Powder X - ray diffraction analysis

Finely crushed grown crystals have been subjected to powder X - ray diffraction using XPERT - PRO diffractometer employing Cu k_α radiations (λ=1.5406 Å). The specimen in the form of a thin film was scanned over 2θ range 10 to 90º at the scan rate of 1^0 /min. The sharp peaks indicate the crystalline nature and all the diffraction planes were indexed using software AUTOX 93. Fig. 3 represents the indexed powder diffraction pattern of grown CLGD crystal.

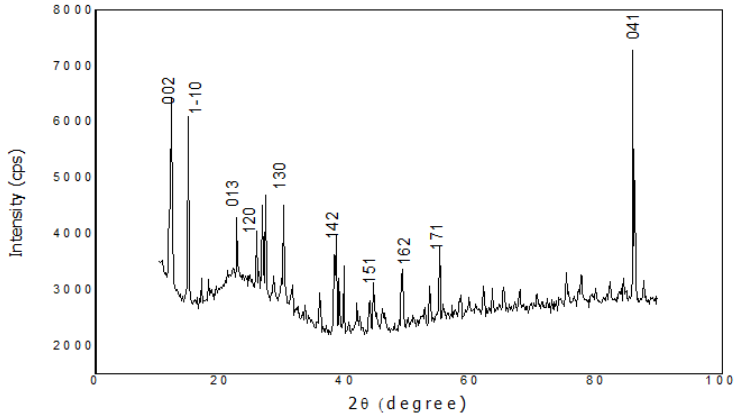

Fig. 3 Powder X – ray diffraction of CLGD

3.3. FT - IR spectral analysis

The FT - IR spectrum of Copper L - Glutamate dihydrate was recorded in the range of 450 - 4000 $cm^{-1}$by Perkin Elmer FT - IR spectrometer to identify presence of various functional groups and it is shown in Figure 4. The observed wavenumbers and assignments are presented in Table 1. The band observed at 483 cm^{-1} is due to the COO^- rocking. The peaks observed at 1131 and 567 cm^{-1} are due to NH_3 rocking and NH_3 torsion modes respectively. C = O bending and asymmetric stretching mode occurs at 1611 and 633 cm^{-1} . C-C-O deformation mode of vibration appears at 758 cm^{-1}. Asymmetric and symmetric stretching modes of C - N are observed at 1395 and 1265 cm^{-1}. Broad peak observed at 3398 and 2322 cm^{-1} was due to OH asymmetric and symmetric stretching vibrations. The N - H bending appeared at the wavenumber 1572 cm^{-1}.

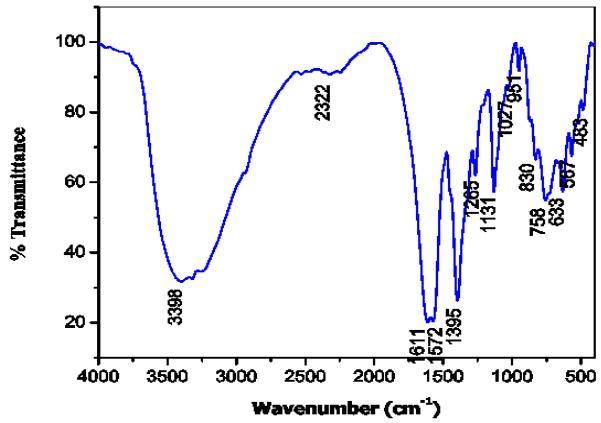

Fig. 4 FT IR spectrum of CLGD

TABLE 2 FT - IR frequency assignments of CLGD single crystal.

FT- IR	Assignment of vibrations
3398	O – H asymmetric stretching
2322	O – H symmetric stretching
1611	C = O asymmetric stretching
1572	N – H bending
1395	C – N asymmetric stretching
1265	C – N symmetric stretching
1131	NH_3 rocking
1027	C – C – N asymmetric stretching
951	C – C stretching
830	C – C symmetric stretching
758	C – C – O deformation
633	C = O bending
567	NH_3 torsion
483	COO rocking

3.4 UV – Vis – NIR Spectral studies

UV-Vis-NIR transmittance and absorption studies have been carried out by using Perkin-Elmer Lambda 35 UV-Vis spectrometer in the spectral region 190 and 1100nm. Optically polished single crystal of thickness 2mm was used to record the spectrum. Figure 5 shows the transmittance and absorbance spectrum of CLGD. The transparency of the crystal is 98% and displays no absorption in the entire UV visible region. The cut-off wavelength of CLGD crystal is observed at 200nm and this is an advantage of amino acid complexes where the absence of strongly conjugated bonds leads to broad transparency range [14]. Knowledge of the optical band gap and extinction coefficient of materials is important parameter for selection of material. The optical absorption coefficient (α) is calculated from the relation $\alpha = (1/t) \log (1/T)$, where T is the transmittance and t is the thickness of the crystal.

The direct band gap of the crystal can be obtained from the absorption coefficient (α) using the relation $\alpha h\gamma = A(h\gamma - Eg)^{1/2}$, where Eg is the optical band gap energy of the crystal, h is the Plank's constant, γ is the frequency and A is a constant. Fig. 6 depicts the variation of $(\alpha h\gamma)^2$ versus photon energy hγ. The band gap was estimated by extrapolating the linear portion near the onset of absorption edge. The band gap energy of CLGD is 5.21eV. The absorption coefficient (α) is related to the extinction coefficient K by the relation $K = \alpha\lambda/(4\pi)$. Figure 7 shows the variation of extinction coefficient of the grown crystal. The extinction coefficient sharply decreases and saturates at 300 nm.

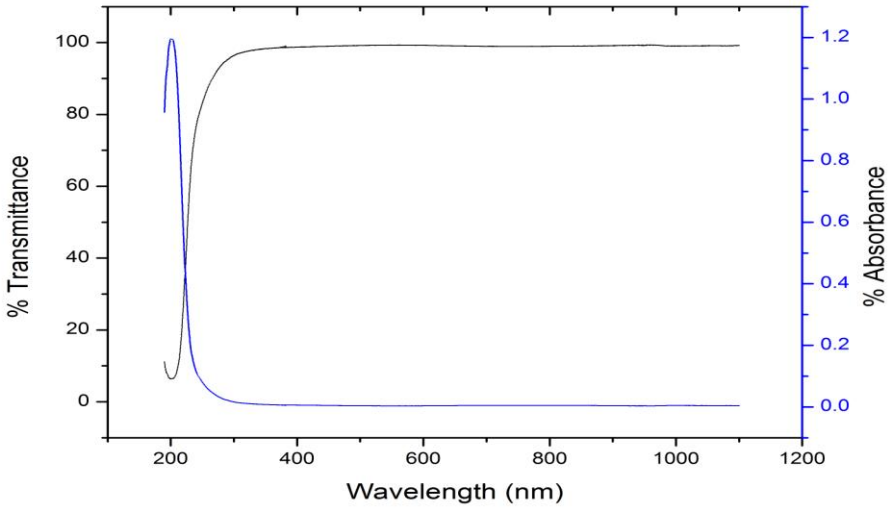

Fig. 5 UV- Vis - NIR spectrum of CLGD.

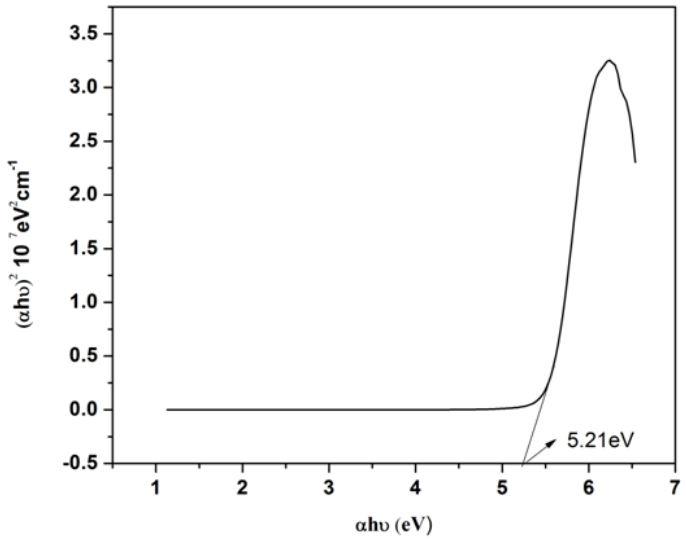

Fig. 6 Energy band gap of CLGD

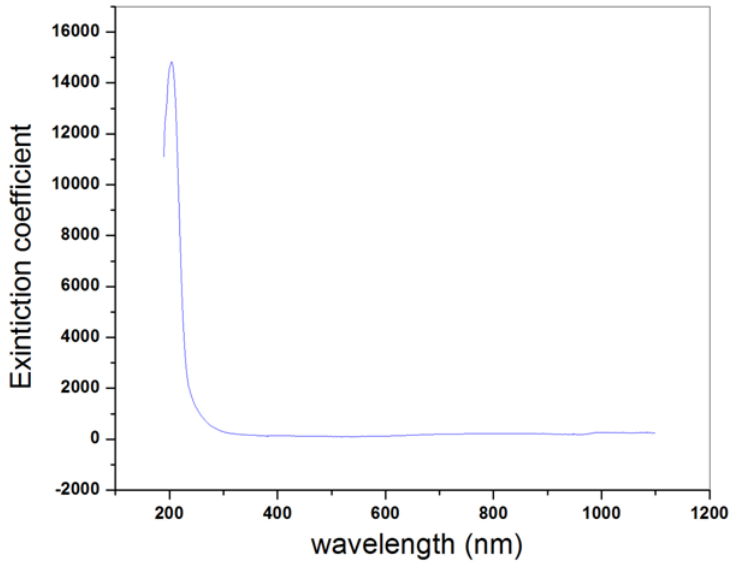

Fig. 7 Extinction coefficient Vs wavelength for CLGD

3.5 Photoluminescence Analysis

Photoluminescence is an elegant tool for characterizing defects, vacancies and other imperfections in the grown crystal. Photoluminescence spectrum was recorded in the wavelength range from 500nm to 600nm using Jasco PL spectrometer. On applying the excitation wavelength 275 nm (4.517 eV) the electronic emission started at 2.91eV and ends at 2.311eV. Hence total energy is emitted with an emission period $0.122X10^{-12}$ s. Photoluminescence emission spectra of CLGD is shown in Fig. 8. The emission peak observed at 553.55 nm (2.244 eV) which is in green region in the electromagnetic spectrum. The band width of this emission spectrum is $2377.21X10^{10}$ Hz. This low bandwidth with sharp peak is the characteristics of radiation transitions at deep neutral defects and good crystalline nature. The relaxation time of CLGD crystal is $1.6\ X10^{-14}$s. The energy band gap of CLGD crystal was calculated using the formula $Eg = 1240/\lambda_{max}$ (eV) where λ is the emission peak wavelength. The energy gap (Eg) of the crystal is 2.378 eV, hence CLGD will be used as insulating material.

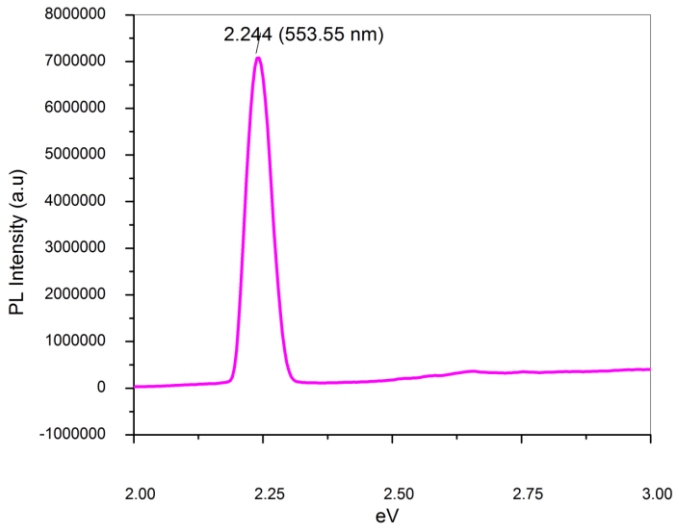

Fig. 8 Photoluminescence spectrum of CLGD

3.6 Dielectric properties

Dielectric constant (ε_r) and dielectric loss (tan δ) are the basic electrical properties of the solids. The single crystal of CLGD of dimensions (4x4) mm^2 in surface area and 2mm thickness of the crystal was smoothly polished using alumina. The opposite faces of the sample were coated with silver paste. A two terminal copper electrode was used as sample holder and the sample was held between the electrodes. Hence the parallel plate capacitor was formed. Hioki LCR dielectric meter working in the range of 10 – 8MHz and a microprocessor supported furnace fitted with a temperature controller was used for dielectric measurements. The variation of capacitance with reference to varying frequencies and dielectric loss measurements were made in the frequency range 50 – 5000 kHz at different temperature. Four type of polarization usually contribute to the dielectric polarization of any ferroelectric material. They are electronic, ionic, dipolar and space charge polarization ($\alpha_t = \alpha_i + \alpha_e + \alpha_o + \alpha_s$). The space charge contribution depends on the purity and perfection of the grown crystals. The contribution of space charge polarization at lower temperature and higher frequencies are negligible. However it is significant at low frequencies. Electronic polarization occurs at very high frequencies. Space charge and dipolar polarization are relaxation processes and are strongly temperature dependent while as ionic and electronic polarization are resonance process and are temperature independent. The dielectric constant is calculated using the relation $\varepsilon_r = Cd / (A\varepsilon_o)$. Where C is the capacitance (F), t the thickness, A the area (m^2) and ε_o the absolute permittivity in the free space having the value of 8.854×10^{-12}F/m. The variation of dielectric constant with frequency of the applied a.c. field is shown in figure 9. In the lower frequency region (0 - 1000Hz) the dielectric constant decreases as the frequency increases. In the higher frequency region the dielectric constant attains saturation. In the higher frequency range the dielectric constant almost remains unaffected by input a.c field. It is clear from this curve that the dielectric constant and dielectric loss of the material strongly dependent on both temperature as well as frequency. Figure 10 shows the dependency of the dielectric loss on frequency. The dielectric loss decreases with increase in frequency.

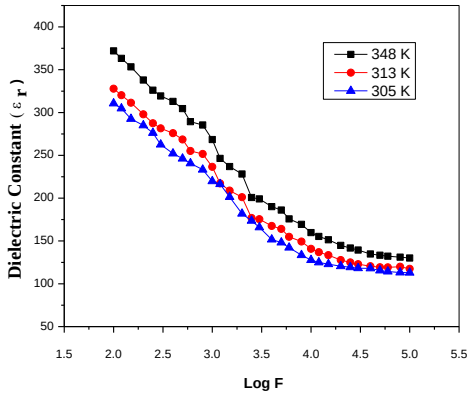

Fig. 9 Dielectric constant as a function of log frequency

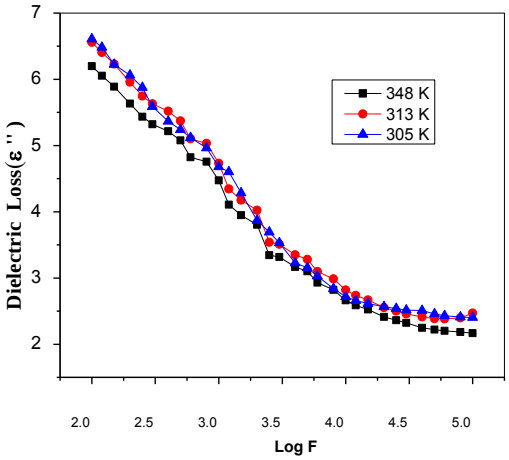

Fig. 10 Dielectric loss versus frequency

The variation of dielectric constant with temperature at four different frequencies 50 kHz to 150 kHz is shown in Figure11.

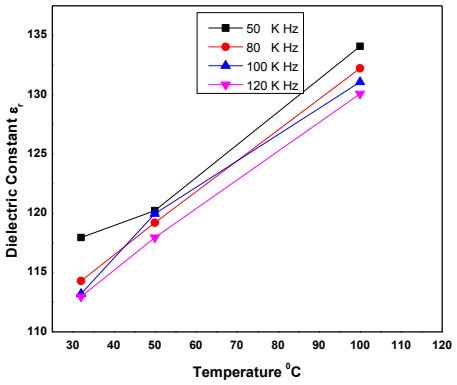

Fig. 11 Temperature vs dielectric constant

The dielectric constant increases as the temperature increases. The rate of variation of dielectric loss with temperature is shown in Figure 12 at four different frequencies. Dielectric loss also exhibits similar behavior as the frequency of the applied field increases. The relaxation time is the time taken by the electron from disturbed position to equilibrium position in the presence of an electric field. Also the decrease of dielectric constant and dielectric loss with increase in frequency suggests that the grown crystal seems to contain molecules of varying relaxation times. At higher frequencies relaxation time is large, hence molecules not able to respond with frequency so the dielectric constant and dielectric loss were low.

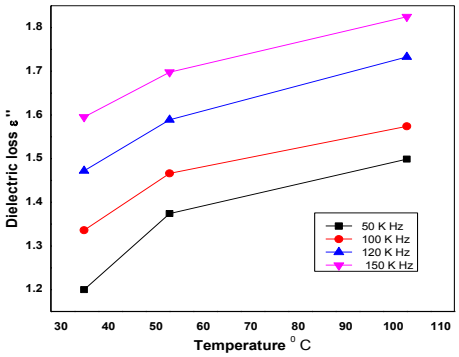

Fig. 12 Temperature vs dielectric loss

3.6 Thermal analysis

Thermo gravimetric analysis (TGA) and differential thermal analysis (DTA) are very important characteristic techniques is used to reveal the thermal stability of the crystal. TG/DTG and DTA curves (Fig. 13) were recorded for copper L - glutamate dihydrate crystal using Perkin Elmer thermal analyzer in the range of temperature from 25 ºC to 1000 ºC at a heating rate of 10 ºC/min in nitrogen atmosphere. Ceramic crucible was used for heating the sample. The initial mass of the material subjected to analysis was 9.9290 mg. Two weight losses were observed in the TGA curve. The material was stable up to 80.58 °C and then weight loss takes place. The first step of weight loss takes place between the temperature 80.58 ºC and 184.02 ºC. In this stage hydroxide group is removed. Second step of decomposition is observed between the temperature 220.57 ºC and 1000 ºC. During this stage L-glutamic acid is removed. The DTA curve clearly follows the TG curve with two peaks. The sharp and well resolved endothermic peaks were observed at 167.58 ºC and 226.38 ºC. The endothermic peak corresponds to the loss of hydroxyl group and L-Glutamic acid.

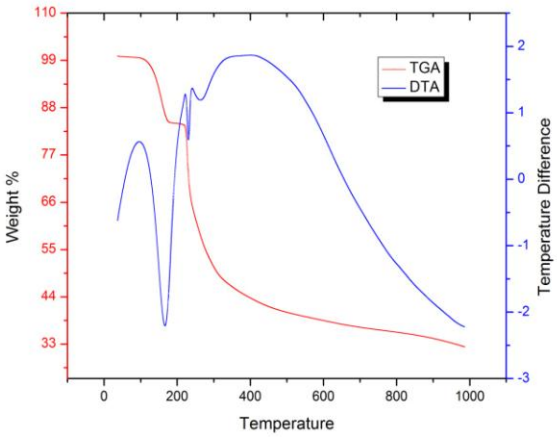

Fig. 13 TGA/DTA spectrum of CLGD

3.7 Differential Scanning Calorimetry

Differential Scanning calorimetric study (DSC) was carried out on a Perkin Elmer DSC 7 Calorimeter with heating rate of 10 ºC / min in nitrogen atmosphere. For this, a small piece of crystal weighting 9.92g was taken. The sample was scanned over the temperature range from 25 to 1000 ºC. The DSC plot shows a sharp peak at 167.58 ºC and highest peak of exothermic at 536.4 ºC. This well-marked endothermic peak is due to the melting point of the compound.

3.8 Microhardness studies

Crystal hardness is a measure of the resistance to the local deformation [15]. The knowledge of hardness is very important and it plays a vital role in device fabrication. Vickers microhardness values were estimated by employing Shimadzu microhardness tester for different loads. The Vickers pyramidal indenter is attached to a microscope with an adopted video camera in order to measure the indentations on a monitor. The dwell time of indentation was kept at 3s. Two indentations were made and the mean values of the two diagonal lengths used for hardness calculation. Vickers microhardness number (H_v) was calculated using the relation $H_v = 1.8544(P/d^2)$ kg/mm^2 where P is the indenter load (kg) and d is the diagonal length of the impression (mm). Fig. 14 shows the variation of Vickers hardness values with applied load. The value increases up to a load of 100g. Cracks develop around the indentation mark above the load of 100g. It is observed from the figure that hardness value is load depending and the value of the hardness increases with increasing load. This phenomenon is called reverse indentation size effect (RISE). To analyze the RISE curve fitting the data according to Meyers [16] law $P = Ad^n$, which correlate the applied load P and its corresponding indentation size d. A is the constant for a given material and n is the Meyers work hardening co-efficient. Figure 15 obtained by plotting log P against log d, the slope of this fit gives "n". The value of n is equal to 2 which means the crystal is soft material characteristic nature according to Onitsch [17]. Since Meyers law is simply an empirical relation, Li and Bradt [18 - 20] proposed a model called Proportional Specimen Resistance (PSR) to explore indentation size effect. To describe the indentation size effect regime we applied the proportional specimen resistance model.

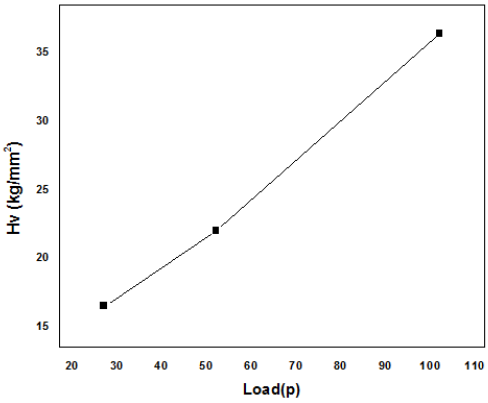

Fig. 14 Hardness behavior of CLGD single crystal.

In the PSR model of Li and Bradt, microhardness can be described by two components, the first term represents the indentation load dependent part and second term represents the load independent part. The indentation test load P is related to the indentation size d as follows.

$$\frac{P}{d} = a_1 + \left(\frac{P_s}{d_s^2}\right) d$$

In the above equation a_1 is the contribution of PSR to the apparent microhardness and a_2 dis the coefficient related to the load dependent microhardness. A plot of P/d against d gives a straight line. The slope of which gives the value of load independent microhardness. Linear regression of P/d versus d confirms the ISE regime. Figure 16 illustrates the load independent part and load dependent part. The slope gives the value of P/d^2 which when multiplied by the Vickers conversion factor 1.8544 gives load independent microhardness. The load independent microhardness value is calculated to be 22.25 g/mm^2. Elastic stiffness constant was computed by Wooster's [21] empirical relation $C_{11} = H_v^{\frac{7}{4}}$. The elastic stiffness increases with increase of load. The calculated stiffness constant for different loads is shown in Table 3.

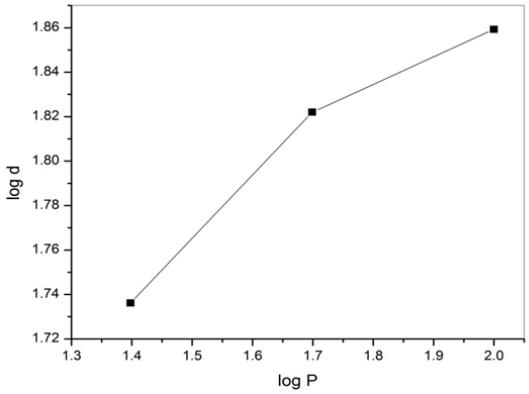

Fig. 15 A plot of log P vs log d.

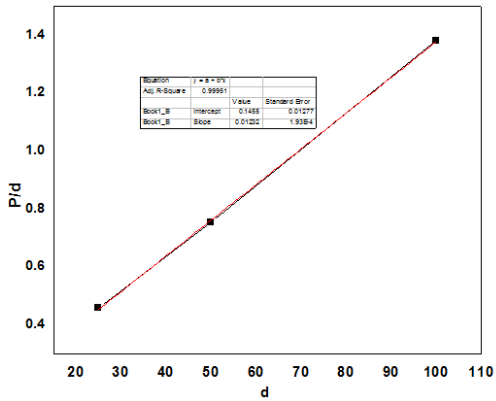

Fig. 16 P/d vs d

TABLE 3 Stiffness Constant of CLGD Crystal

H_v (g/mm^2)	$C_{11} \times 10^{14}$ (N/m^2)
15.5	2.078×10^{14}
20.7	3.44×10^{14}
35.2	8.73×10^{14}

3.9 Etching studies

Etching is a technique which is used to reveal the defects in crystals like dislocations, growth bands, twin boundaries and point defects. Normally when the crystal is dissolved in the solvent, well defined etch pits are formed. The formation of the etch pits are assumed to be the reverse of growth process. The etching features observed on the grown crystal was recorded by high resolution optical polarization microscope. The surface of the crystal was polished well before the etching process. The crystal was dipped in double distilled water and wiped using tissue paper. The etch patterns were recorded using polarization microscope fitted with Motic camera. The photographs were taken with a maximum etching time of 5 seconds. Figure 17 shows the etch patterns observed on the CLGD single crystal. Etch pits and cracks were observed.

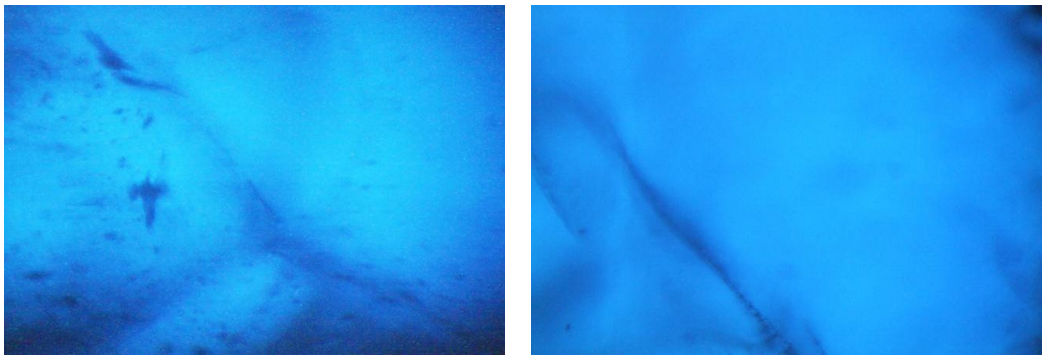

Fig. 17 Etch patterns of CLGD

3.10 SHG Efficiency

The quadratic NLO property was checked and the SHG relative efficiency in the powder material was measured by Kurtz and Perry method [22]. KDP crystal was powdered to the identical size and used as a reference material in the SHG measurement. The crystal was grained into the powder and densely packed in 1.5mm diameter micro capillary tube. The laser energy of 7mJ was applied on the sample there was absence of green radiation energy (532 nm) and SHG signal was very low. So CLGD could not be used in the fabrication of NLO devices.

IV. Figures And Tables

Fig. 1 As grown single crystals of CLGD
Fig. 2 ORTEP diagram of CLGD
Fig. 3 Powder X – ray diffraction of CLGD
Fig.4 FT IR spectrum of CLGD
Fig. 5 UV- Vis - NIR spectrum of CLGD.
Fig. 6 Energy band gap of CLGD
Fig. 7 Extinction coefficient Vs wavelength for CLGD
Fig. 8 Photoluminescence spectrum of CLGD
Fig. 9 Dielectric constant as a function of log frequency
Fig. 10 Dielectric loss versus frequency
Fig.11 Temperature vs dielectric constant
Fig. 12 Temperature vs dielectric loss
Fig. 13 TGA/DTA spectrum of CLGD
Fig.14 Hardness behavior of CLGD single crystal.
Fig. 15 A plot of log P vs log d.
Fig. 16 P/d vs d
Fig. 17 Etch patterns of CLGD
Table 1 Crystal Data and Structure Refinement for CLGD
Table 2 FT - IR frequency assignments of CLGD single crystal.
Table 3 Stiffness Constant of CLGD Crystal

V. Conclusion

CLGD crystals were grown from aqueous solution by slow evaporation method. The crystal structure was elucidated using standard crystallographic procedures. FT-IR spectra revealed the presence of the various functional groups. UV-Vis-NIR study shows that the crystal transparent for the fundamental and second harmonic of Nd:YAG (λ=1064 nm) laser. Thermal analysis reveals that CLGD is thermally stable up to 80 ºC. From Vickers microhardness it was observed that the microhardness values increases with increase of load. The work hardening coefficient n>2 indicates that the crystal belongs to soft material category. The elastic stiffness constant gives an idea of tightness of bonding between the neighboring ions. The dielectric constant and dielectric loss of CLGD crystals dependent on frequency of the applied electric field at different temperature. In the low frequency region both the dielectric constant and dielectric loss decreases sharply.

Acknowledgements

The authors T. B , P.R and P.J would like to acknowledge the CSIR, New Delhi, India for providing financial support [Project ref. No. 03(1314)/14/EMR II dt.16-04-14].The authors gratefully acknowledge the scientific supports extended by Sophisticated Analytical Instrument Facility (SAIF),Indian Institute of Technology Madras, Chennai - 60 0 036, India. The authors acknowledge Prof. P.K. Das, Department of Inorganic and Physical Chemistry, Indian Institute of Science, Bangalore for having extended the laser facilities for the SHG measurement.

References

[1]. J.D. Bernal, Z. Crystallogr. 78 (1931) 363.
[2]. S. Hirokawa, Acta Cryst. 8 (1955) 637.
[3]. E.S.Ferrari, R.J. Davy Cryst. Growth & Des., 2004, 4 (5) 1061– 1068.
[4]. H. Moshe, G.Levi, Y.Mastai, Cryst. Eng. Comm**,** 15 (2013) 9203 - 9209.
[5]. A. Sequeira, H. Rajagopal and R. Chidambaram Acta Crystallogr. B57 (1972) 2514 - 2519.
[6]. Z. Ciunitz and T. Glowiak Acta Crystallogr. C39 (1983) 1271 – 1273.
[7]. J.D. Dunitz & W.B. Schweizer Acta Crystallogr. C51 (1995) 1377 - 1379.
[8]. B. Sridhar, N. Srinivasan and R.K. Rajaram Acta Crystallogr. E58 (2002) o272 – o276.
[9]. J. Uma and V. Rajendran J. Therm. Anal. Calorim. 117 (2014)1157 – 1163.
[10]. R. Sathyalaxmi, V. Kannan, R. Bairava Ganesh, P. Ramasamy Cryst. Res. Technol. 42(1) (2007) 78 – 83.
[11]. S. Kumararaman, K. Kirubavathi and K. Selvaraju Journal of Minerals & Material Characterization and Engineering 10, No.1 (2011) 49 – 57.
[12]. K Selvaraju, R Valluvan and S Kumararaman Materials Letters 60 (13) (2006) 1565-1569
[13]. C. M. Gramaccioli and R. E. Marsh, Acta Cryst.21 (1966)594
[14]. A. Ashour, N. El – Kadry, S. A. Mahmoud, Thin Solid Films 269 (1995) 117 – 120.
[15]. P. Sayan and J. Ulrich Cryst. Res. Tech. 36 (2001) 1253 – 1262.
[16]. E. Meyer, Phys. Z9 (1908) 66.
[17]. E. M. Onitsch, Mikroskopie 2 (1947) 131.
[18]. M. Hanneman, Metall. Manchu 23 (1941) 135.
[19]. Li and R.C. Bradt, J. Mater. Sci. 31(1996) 1065 – 1070.
[20]. F. Frohlich, P. Grau and W. Grellmann, Phys. Status Solidi 42 (1977) 79 – 83.
[21]. B.W. Mott, Micro indentation Hardness Testing: Butterworths, London, 1956.
[22]. W.A. Wooster, Rep. Progr. Phys. 16 (1953) 62 – 82.

IOSR Journal of Applied Physics (IOSR-JAP) is UGC approved Journal with Sl. No. 5010, Journal no. 49054.

S. Sakthivel. "Growth, Structural, Optical, Thermal and Mechanical properties of Copper Glutamate Dihydrate Single crystal." IOSR Journal of Applied Physics (IOSR-JAP), vol. 9, no. 4, 2017, pp. 57–67.